Thermal charge carrier driven noise in transmissive semiconductor optics

F. Bruns,[1] S. P. Vyatchanin,[2] J. Dickmann,[3] R. Glaser,[4] D. Heinert,[4] R. Nawrodt,[5] and S. Kroker[3,1]

[1]*Technische Universität Braunschweig, LENA Laboratory for Emerging Nanometrology, Pockelsstraße 14, 38106 Braunschweig, Germany*

[2]*Faculty of Physics, M. V. Lomonosov Moscow State University, Moscow 119991, Russia and Quantum Technology Centre, M. V. Lomonosov, Moscow State University, Moscow 119991, Russia*

[3]*Physikalisch-Technische Bundesanstalt, Bundesallee 100, 38116 Braunschweig, Germany*

[4]*Institut für Festkörperphysik, Friedrich-Schiller-Universität Jena, 07743 Jena, Germany*

[5]*Physikalisches Institut, Universität Stuttgart, 70569 Stuttgart, Germany*

(Received 12 March 2020; accepted 26 June 2020; published 10 July 2020)

Several sources of noise limit the sensitivity of current gravitational wave detectors. Currently, dominant noise sources include quantum noise and thermal Brownian noise, but future detectors will also be limited by other thermal noise channels. In this paper, we study a thermal noise source which is caused by spatial charge carrier density variations in semiconductor materials. We provide an analytical model for the understanding of charge carrier fluctuations under the presence of screening effects and show that charge carrier noise will not be a limiting noise source for third-generation gravitational wave detectors.

DOI: 10.1103/PhysRevD.102.022006

I. INTRODUCTION

Gravitational wave detection [1,2] is an exciting and growing field in the realm of high-precision metrology. For the first detection of a gravitational wave, complex infrastructure was built, taking huge care to reduce all of the possible noise sources. In particular, the fascinating accuracy of a displacement measurement of a macroscopic test mass is demonstrated on a level of about $\sim 10^{-18}$ m [3–8].

A third generation of gravitational wave detectors is planned in order to access gravitational waves as a new channel of information into the Universe, addressing fundamental questions such as the nature of dark matter, the inner structure of black holes, and the origin of the Universe itself [9]. For third-generation gravitational wave detectors (Einstein Telescope in Europe or Voyager and Cosmic Explorer in USA), the use of crystalline materials is considered [10]. Third-generation gravitational wave detectors are severely limited by thermal noise. Therefore, there is a high probability that they will be run at cryogenic temperatures. At these temperatures, crystalline materials have superior mechanical quality factors compared to conventional amorphous materials, thus being less susceptible to thermal Brownian noise [11–16]. Therefore, semiconductors such as silicon are considered as possible substrate materials. This class of materials is potentially susceptible to novel noise channels.

In this paper, we study thermal carrier noise in semiconductor materials. Similarly to thermochemical noise [17], which is caused by the diffusion of optical impurities, this source of noise originates from the thermal motion of free charge carriers in the transmissive optical elements. The Brownian motion of charge carriers leads to spatial variations of the free carrier density, thus creating local fluctuations of the refractive index. These fluctuations will be probed by any beam of light transmitted through the optical element. Below, we refer to this noise as thermal charge carrier refractive (TCCR) noise. For free charge carriers, screening effects have to be considered which distinguish TCCR noise from thermochemical noise. A quantitative analysis of TCCR noise is presented, taking into account Debye screening which depresses TCCR noise.

II. PROBLEM STATEMENT

Earthbound gravitational wave detectors consist of a large-scale Michelson interferometer with Fabry-Perot (FP) cavities in the arms for signal enhancement [18]. An incoming gravitational wave with the strain h displaces the end mirrors of the FP cavities by a length of δl:

$$\delta l = \frac{L_0 h}{2}. \tag{1}$$

Here, L_0 denotes the undisturbed arm length. In order to measure the variation of the gravitational metric h, the displacement of the end mirrors is probed with a laser beam. The displacement of the end mirrors causes a phase shift between the interferometer arms which is enhanced by the FP cavities and read out via interference of the laser light of the two arm cavities.

In this paper, we investigate transmissive optics made of semiconductor materials which is particularly important for third-generation gravitational wave detectors such as the

Einstein Telescope (ET). In semiconductor optics such as silicon [19], free charge carriers are present. These charge carriers move thermally akin to Brownian motion, thus creating local charge carrier density fluctuations η. As stated by Soref and Bennett [20], the refractive index n is dependent on the charge carrier concentration as an effect of the free carrier dispersion:

$$\delta n = \beta\eta, \qquad \beta = \frac{-e^2}{2\epsilon_0 n\omega_l^2 m_e}, \tag{2}$$

with ω_l the laser frequency, n the refractive index of the semiconductor, e the elementary charge, and m_e the effective mass of majority charge carriers. That is why the local charge carrier fluctuations η cause fluctuations of the refractive index δn. These fluctuations are probed by any laser beam propagating through the optical element.

When a Gaussian laser beam propagates a distance L along the z axis inside of, e.g., the input mirror (test mass) of a FP cavity (see Fig. 1), it reads out the information on the variation of the refractive index inside the input test mass weighted by the light intensity distribution in the cross section. Hence, the optical path length of the laser beam is shifted by a value of ξ:

$$\xi(t) = \beta \int \eta(\vec{r}, t) \cdot \Psi(\vec{r}) d\vec{r}, \tag{3}$$

$$\Psi(\vec{r}) = \begin{cases} \frac{e^{-(x^2+y^2)/r_0^2}}{\pi r_0^2}, & \text{if } |z| \le \frac{L}{2}, \\ 0, & \text{if } |z| > \frac{L}{2}, \end{cases} \tag{4}$$

where L is the length of the mirror substrate, r_0 is the Gaussian radius of the light beam (referring to the length where the amplitude falls off by e^{-1}), x and y are the transversal coordinates, and $\int d\vec{r}$ is an integration over the volume of the input test mass. In the measurement, we cannot distinguish between a fluctuation of the optical path length caused by noise or a length shift of the mirror caused by a gravitational wave. In this way, carrier density fluctuations η inside transmissive semiconductor optics contribute to the measured strain as h_ξ:

$$\eta \to \xi \to h_\xi.$$

We call this noise TCCR noise. In order to quantify TCCR noise, we have to model the carrier density fluctuations under consideration of screening effects that occur for free charge carriers (Sec. II B). Furthermore, we have to understand how a change in the optical path length ξ is related to the strain h caused by the gravitational wave (Sec. II A) and combine both to get an expression for the amplitude of TCCR noise (Sec. II C). Finally, we use this to explicitly compute the TCCR noise of ET input test masses (Sec. III).

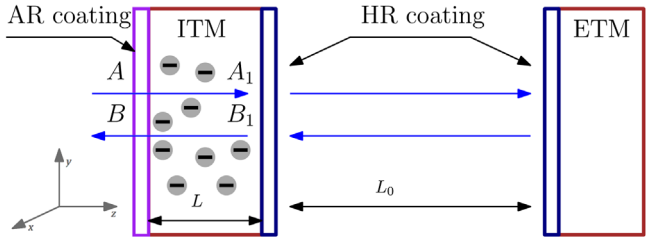

FIG. 1. Fabry-Perot cavity. The surfaces of the input test mass are covered by antireflecting (AR) and high-reflecting (HR) coatings. The thermal motion of carriers in the input test mass produces additional fluctuations of the refractive index which are probed by the transmitted beams. The position of the coordinate system has been shifted for better visibility. Its center is actually at the center of mass of the input mirror.

A. Coupling of noise-induced changes in the path length and the measured strain

For simplicity reasons, we consider a Michelson configuration with interferometer arms perpendicular to each other. To establish our model for TCCR noise, we examine a FP cavity with mirrors as free test masses as shown in Fig. 1. TCCR noise in the input test mass disturbs the optical path length nL by a value of ξ. From input-output relations, we can see that the reflected amplitude B (see notations in Fig. 1) contains an additional fluctuation term in the frequency domain:

$$b_\xi = \frac{\gamma + i\Omega}{\gamma - i\Omega} \cdot Aik\xi + Aik\xi = Aik\xi \cdot \frac{2\gamma}{\gamma - i\Omega}, \tag{5}$$

where Ω is a spectral frequency, A is the amplitude of the incoming light, $\gamma = T^2/2\tau$ is the amplitude relaxation rate of the FP cavity, $\tau = 2L_0/c$ is the round trip time (usually $\Omega\tau \ll 1$), and T and R are the amplitude transmittance and reflectance, respectively, of the input test masses ($R^2 + T^2 = 1$; we assume $T \ll 1$). The two terms in the first equation of (5) describe the perturbation created in the incident wave (after circulation inside the cavity) and the directly reflected one, respectively. Effectively, the cavity acts as a low-pass Lorentz filter.

The fluctuation term should be compared with the signal term b_s produced by the displacement $\delta L = L_0 h_s/2$ (h_s is the perturbation of the metric caused by the gravitational wave):

$$b_s = T \cdot \frac{2A}{T} \cdot \frac{2ik\delta L}{1 - Re^{i\Omega\tau}} = \frac{2A \cdot ikL_0}{\tau(\gamma - i\Omega)} \cdot h_s. \tag{6}$$

In gravitational wave detectors of the third generation, there are FP cavities in the east and north arms, and the light from them interferes on a 50/50 beam splitter. Thus, the signal b_s (6) of the gravitational wave is increased by a factor of $\sqrt{2}$:

$$b_s^{\mathrm{ET}} \Rightarrow b_s\sqrt{2}. \tag{7}$$

On the other hand, there are fluctuations ξ_n and ξ_e in the input test masses of the north and east arm cavities. As follows,

$$b_\xi^{\mathrm{ET}} = Aik \cdot \frac{2\gamma}{\gamma - i\Omega} \cdot \xi_{\mathrm{ET}}, \qquad \xi_{\mathrm{ET}} = \frac{\xi_e + \xi_n}{\sqrt{2}}. \tag{8}$$

Note that the fluctuations ξ_e and ξ_n do not depend on each other and have equal power spectral densities. The power spectral density of ξ_{ET} is equal to the power spectral density of ξ_e (or ξ_n). Comparing (5) and (6) by taking into account (7) and (8), one can find that the variation of the gravitational metric h and the optical path fluctuations ξ are related as

$$h = h_s + h_\xi, \qquad h_\xi = \frac{\gamma\tau}{\sqrt{2}} \cdot \frac{\xi_{ET}}{L_0} = \frac{\pi}{\sqrt{2}F} \cdot \frac{\xi_{ET}}{L_0}, \tag{9}$$

with F the finesse of the Fabry-Perot cavity.

B. Thermal charge carrier density fluctuations

As suggested by the fluctuation-dissipation theorem, we have to understand the dissipation mechanism (in our case, that is diffusion) to describe fluctuations of charge carriers. For this reason, we derive a diffusion equation including screening effects. We expect Debye screening to suppress diffusion processes, thus reducing the fluctuations in the optical elements. Because of the residual doping in the large test mass substrates required for gravitational wave (GW) detection, a majority charge carrier is present [21]. Without loss of generality, we assume electrons to be the majority charge carriers. We start with the continuity equation for the carrier concentration n_{cc} [22]:

$$\frac{\partial n_{cc}}{\partial t} = -\vec{\nabla} \cdot \vec{J}, \tag{10}$$

where $\vec{J}$ is the current density described by [22]

$$\vec{J} = -D\vec{\nabla} n_{cc} + n_{cc}\mu\vec{E}, \tag{11}$$

$$\mu = \frac{eD}{k_B T}. \tag{12}$$

Here D is the diffusion coefficient, μ the carrier mobility, e the carrier charge, k_B the Boltzmann constant, and T the temperature. The last term in (11), which is proportional to a small electric field $\vec{E}$, is introduced to account for Debye screening. The carrier concentration n_{cc} can be described as a sum of a large constant n_0 and a small fluctuating part η:

$$n_{cc} = n_0 + \eta, \qquad n_0 = \frac{1}{e\mu\rho_e}, \tag{13}$$

with the electrical resistivity ρ_e. The screening electric field $\vec{E}$ is given by the Poisson equation [22]:

$$\vec{\nabla} \cdot \vec{E} = \frac{en_{cc}}{\epsilon\epsilon_0} \simeq \frac{e\eta}{\epsilon\epsilon_0}. \tag{14}$$

Here $\epsilon = n^2$ with n the refractive index and ϵ_0 the vacuum permittivity. After substituting (11) into (10) while using (13), we get

$$\frac{\partial \eta}{\partial t} = D\Delta\eta - n_0\mu\vec{\nabla} \cdot \vec{E}. \tag{15}$$

Since η is a small deviation from thermal equilibrium (i.e., a fluctuation), we have neglected any quadratic term of η. Finally, we get a diffusion equation utilizing (14):

$$\frac{\partial \eta}{\partial t} = D\left(\Delta\eta - \frac{1}{\ell_D^2}\eta\right), \qquad \ell_D = \sqrt{\frac{\epsilon\epsilon_0 k_B T}{n_0 e^2}}. \tag{16}$$

Here $\Delta = (\vec{\nabla})^2$ is the Laplace operator and ℓ_D is the Debye length. Compared to conventional diffusion equations there is an additional term, $-D\eta/\ell_D^2$, which is a direct consequence of screening effects under the assumption of only having small deviations from thermal equilibrium η.

Next we want to include fluctuations. In the frame of the Langevin approach [23,24], we introduce the Langevin forces $F(\vec{r}, t)$ into the right part of (16):

$$\frac{\partial \eta}{\partial t} = D\left(\Delta\eta - \frac{1}{\ell_D^2}\eta\right) + F(\vec{r}, t). \tag{17}$$

These Langevin forces $F(\vec{r}, t)$ cause the Brownian movement of the charge carriers. They are uncorrelated representing white Gaussian noise:

$$\langle F(\vec{k}, \omega)F^*(\vec{k}', \omega')\rangle = (2\pi)^4 F_0^2(k^2 + \ell_D^{-2}) \times \delta(\vec{k} - \vec{k}')\delta(\omega - \omega'). \tag{18}$$

The correlators of the fluctuation forces and the constant F_0 should be chosen to fulfill the equation

$$\langle \eta^2 \rangle = \frac{n_0}{V}, \tag{19}$$

which corresponds to the well-known requirement (of a Poisson process) that the variation $\langle \Delta N^2 \rangle$ of the particle number in a volume V is equal to the mean particle number: $\langle \Delta N^2 \rangle = \langle N \rangle$ [25]. From (19), one can find

$$F_0^2 = 2Dn_0. \tag{20}$$

Now we can calculate the autocorrelation function of density fluctuations:

$$B(\vec{\rho},\tau) \equiv \langle \eta(\vec{r},t)\eta(\vec{r}-\vec{\rho},t-\tau)\rangle = \frac{2Dn_0}{(2\pi)^4}\int d\vec{k}d\omega \frac{(k^2+\frac{1}{\ell_D^2})e^{i\omega\tau+i\vec{k}\vec{\rho}}}{D^2(k^2+\frac{1}{\ell_D^2})^2+\omega^2}. \quad (21)$$

From that, the *double-sided* power spectral density (PSD) $S_{\eta\eta}(\vec{k},\omega)$ can be found using the Wiener-Khinchin theorem [26]:

$$S_{\eta\eta}(\vec{k},\omega) = \int B(\vec{\rho},\tau)e^{-i\omega\tau-i\vec{k}\vec{\rho}}d\vec{\rho}d\tau = n_0\cdot\frac{2D(k^2+\frac{1}{\ell_D^2})}{D^2(k^2+\frac{1}{\ell_D^2})^2+\omega^2}. \quad (22)$$

C. Variations of the optical path length

Now that we know the spectral noise density of charge carrier fluctuation (22) and how a shift of the optical change of path length relates to the gravitational strain (9), we can combine these two results with the readout of the Gaussian beam (3) to get the measurable TCCR noise in a gravitational wave detector. The readout of the Gaussian beam, Eq. (3), can be rewritten as

$$\xi(t) = \beta\int\frac{d\vec{k}d\omega}{(2\pi)^4}\eta(\vec{k},\omega)\Psi(\vec{k})e^{i\omega t}, \quad (23)$$

where $\eta(\vec{k},\omega)$ and $\Psi(\vec{k})$ are Fourier transforms of $\eta(\vec{r},t)$ and $\Psi(\vec{r})$, respectively. To get the PSD of ξ we calculate the autocorrelation function of ξ:

$$\langle\xi(t)\xi(t-\tau)\rangle = \beta^2\int\frac{d\vec{k}d\omega}{(2\pi)^4}\frac{d\vec{k}'d\omega'}{(2\pi)^4} \times\langle\eta(\vec{k},\omega)\eta^*(\vec{k}',\omega')\rangle\Psi(\vec{k})\Psi^*(\vec{k}')e^{i\omega t-i\omega'(t-\tau)}. \quad (24)$$

Using (18), we can express the correlator as

$$\langle\eta(\vec{k},\omega)\eta^*(\vec{k}',\omega')\rangle = \frac{(k^2+\frac{1}{\ell_D^2})}{\omega^2+D^2(k^2+\frac{1}{\ell_D^2})^2} \times(2\pi)^4F_0^2\cdot\delta(\vec{k}-\vec{k}')\delta(\omega-\omega'), \quad (25)$$

and substituting into (24) and using the Wiener-Khinchin theorem and the normalization (20), we write down the double-sided PSD $S_{\xi\xi}(\omega)$:

$$S_{\xi\xi}(\omega) = 2Dn_0\beta^2\int\frac{d\vec{k}}{(2\pi)^3}\cdot\frac{(k^2+\frac{1}{\ell_D^2})|\Psi(\vec{k})|^2}{\omega^2+D^2(k^2+\frac{1}{\ell_D^2})^2}. \quad (26)$$

With the results of Sec. II A, we can rewrite (26) in terms of the GW metric using (9):

$$S^h_{\xi\xi}(\omega) = \frac{n_0\beta^2(\gamma\tau)^2}{L_0^2}\int\frac{d\vec{k}}{(2\pi)^3}\cdot\frac{D(k^2+\frac{1}{\ell_D^2})|\Psi(\vec{k})|^2}{\omega^2+D^2(k^2+\frac{1}{\ell_D^2})^2}. \quad (27)$$

In the usual case, when the Debye length is much smaller than the physical dimensions of the systems, i.e., the Gaussian radius and the length of the substrate (see Table II), $\ell_D \ll r_0, L$ this expression can be simplified:

$$S^h_{\xi\xi}(\omega) = \frac{n_0\beta^2(\gamma\tau)^2}{L_0^2}\cdot\frac{L}{2\pi r_0^2}\cdot\frac{\tau_m}{1+\omega^2\tau_m^2}, \quad (28)$$

$$\tau_m = \frac{\ell_D^2}{D} = \epsilon\epsilon_0\rho, \quad (29)$$

where τ_m is the Maxwell relaxation time. Here we used the normalization

$$\int\frac{d\vec{k}}{(2\pi)^3}|\Psi(\vec{k})|^2 = \int d\vec{r}|\Psi(\vec{r})|^2 = \frac{L}{2\pi r_0^2}. \quad (30)$$

The PSD can be converted into the amplitude spectral density (ASD):

$$S^h_\xi(\omega) = \sqrt{S^h_{\xi\xi}(\omega)}. \quad (31)$$

Note that formula (27) for the spectral noise density is valid for frequencies smaller than the inverse diffusion time, because the equation of motion (15) does not account for retardation effects. The diffusion time is determined by either the Maxwell relaxation time or the electron lifetime, whatever is smaller [27]. In silicon, which is an indirect semiconductor, the diffusion time is given by the Maxwell relaxation time (29), which is around 10^{-8} s for pure silicon at room temperature. The limiting frequency is, therefore, around 10^8 Hz, which is much larger than the frequency range of third-generation gravitational wave detectors of 1–10^4 Hz [19].

III. COMPUTATION OF TCCR NOISE

To quantify the magnitude of TCCR noise, we are going to use the low-frequency interferometer of the Einstein Telescope [19] as an example for a cryogenically operated third-generation gravitational wave detector, where the use of crystalline substrate materials is considered. Since we are examining transmissive TCCR noise, the HR and AR coatings do not contribute significantly because of their small thickness. In amorphous coatings, TCCR noise is even further reduced due to the low amount of free charge carriers.

TCCR noise is dependent on the diffusion coefficient D and the Debye length ℓ_D (see Table II for numerical values of D and ℓ_D). This is why it is indirectly also a function of temperature T and doping density n_D. At this time, large

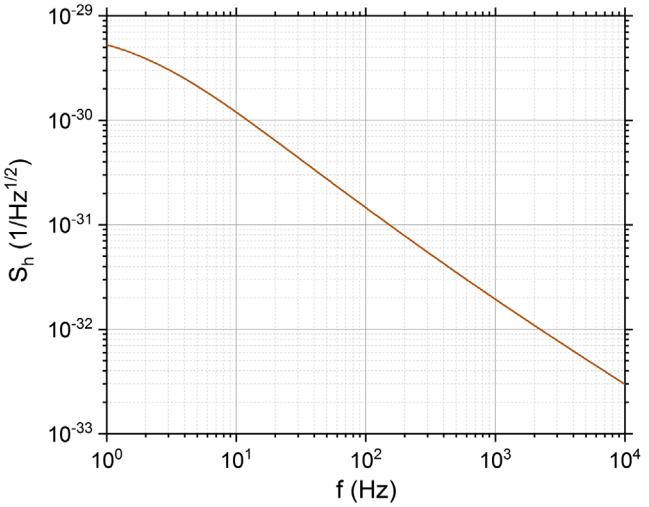

FIG. 2. ASD of TCCR noise in the input test mass substrates of ET at 10 K for pure Si, $n_D = 5 \times 10^{12}\ \frac{1}{\mathrm{cm}^3}$. The ASD falls off with f^{-1} akin to a Brownian noise source. The frequency-independent, approximated formula (28) cannot be used in this case because of the freeze-out of charge carriers enabling the Debye length to become of the order of the Gaussian beam radius (see Table II).

high-purity silicon samples can be produced with the magnetically assisted Czochralski technique with a resistivity of up to 10 kΩ cm. To account for production difficulties, we are looking at n-type silicon with a worse resistivity of 1 kΩ cm, which corresponds to a doping density of around $4.4 \times 10^{12}\ \frac{1}{\mathrm{cm}^3}$, which is equivalent to a resistivity of 1 kΩ cm at room temperature [21]. In order to calculate the mean carrier density n_0 as a function of the doping density, a model for semiconductors with no compensation (no acceptors) has been used [28]:

$$n_0 = \frac{2n_D}{1 + \left[1 + 4g_D \frac{n_D}{n_c} \exp\left(\frac{E_D^b}{k_B T}\right)\right]^{1/2}}. \tag{32}$$

Here g_D is the donor degeneracy, n_D is the donor concentration, E_D^b is the energy gap between donor level and the conduction band, and n_c is the conduction band edge density:

$$n_c = 2\left(\frac{m_{e,b}^* k_B T}{2\pi\hbar^2}\right)^{3/2}, \tag{33}$$

with $m_{d,e}^*$ the effective density-of-states mass of the conduction band electrons. As dopants, we considered shallow phosphorous donors which have a degeneracy of $g_D = 2$ and an energy gap of $E_D^b = 45$ meV.

Additionally, we want to be able to model the diffusion coefficient D. For this, we used the Einstein-Smoluchowski equation in order to replace the diffusion coefficient D with the well-investigated charge carrier mobility μ [28]:

$$D = \frac{k_B T}{e}\mu. \tag{34}$$

A more precise expression for D can be obtained from taking into account the carrier band curvature. In our case, though, the Fermi level is several eV deep within the band

TABLE I. Parameters of the input test masses of the Einstein Telescope (p. 347 in Ref. [19]).

Parameter	Symbol	Value
Finesse of FP cavity	F	880
Mirror thickness	L	0.5 m
Gaussian radius	r_0	0.09 m
Laser wavelength	λ_L	1550 nm
Arm length	L_0	10^4 m
Refractive index Si [32]	n	3.487
Effective electron mass Si	m_e	$0.260 m_0$
Electron rest mass	m_0	9.109×10^{-31} kg
Boltzmann constant	k_B	1.380×10^{-23} J/K
Vacuum permittivity	ϵ_0	8.854×10^{-12} AS/Vm

TABLE II. Electron mobility μ, diffusion coefficient D, and Debye length ℓ_D of Si at different temperatures. The mobility data of Si at 126 K have been approximated by taking the mean of the mobilities at 100 and 150 K from Li and Thurber [30].

		Silicon		
$T[K]$	$n_D\ [1/\mathrm{cm}^3]$	$\mu\ [\mathrm{m}^2/\mathrm{Vs}]$	$D\ [\mathrm{m}^2/\mathrm{s}]$	$\ell_D\ [\mathrm{m}]$
10	5×10^{12}	38.8 [29]	3.34×10^{-2}	9.38×10^{-2}
77	10^{14}	2.04 [30]	1.35×10^{-2}	6.84×10^{-7}
77	5×10^{14}	1.55 [30]	1.03×10^{-2}	4.51×10^{-7}
77	10^{15}	1.31 [30]	8.67×10^{-3}	3.78×10^{-7}
77	5×10^{15}	0.845 [30]	5.61×10^{-3}	2.52×10^{-7}
77	10^{16}	0.655 [30]	4.35×10^{-3}	2.12×10^{-7}
77	5×10^{16}	0.287 [30]	1.90×10^{-3}	1.41×10^{-7}
77	10^{17}	0.184 [30]	1.22×10^{-3}	1.19×10^{-7}
77	5×10^{17}	0.050 [30]	3.32×10^{-4}	7.94×10^{-8}
77	10^{18}	0.027 [30]	1.82×10^{-4}	6.67×10^{-8}
126	10^{14}	1.09	1.19×10^{-2}	4.19×10^{-7}
126	5×10^{14}	0.895	9.72×10^{-3}	2.61×10^{-7}
126	10^{15}	0.795	8.63×10^{-3}	2.15×10^{-7}
126	5×10^{15}	0.557	6.05×10^{-3}	1.41×10^{-7}
126	10^{16}	0.456	4.95×10^{-3}	1.18×10^{-7}
126	5×10^{16}	0.224	2.43×10^{-3}	7.81×10^{-8}
126	10^{17}	0.150	1.63×10^{-3}	6.55×10^{-8}
300	10^{14}	0.146 [30]	3.76×10^{-3}	4.33×10^{-7}
300	5×10^{14}	0.138 [30]	3.56×10^{-3}	2.14×10^{-7}
300	10^{15}	0.137 [30]	3.54×10^{-3}	1.64×10^{-7}
300	5×10^{15}	0.129 [30]	3.32×10^{-3}	9.52×10^{-8}
300	10^{16}	0.121 [30]	3.13×10^{-3}	7.73×10^{-8}
300	5×10^{16}	0.092 [30]	2.38×10^{-3}	4.93×10^{-8}
300	10^{17}	0.075 [30]	1.93×10^{-3}	4.10×10^{-8}
300	5×10^{17}	0.043 [30]	1.11×10^{-3}	2.70×10^{-8}
300	10^{18}	0.030 [30]	7.74×10^{-4}	2.26×10^{-8}

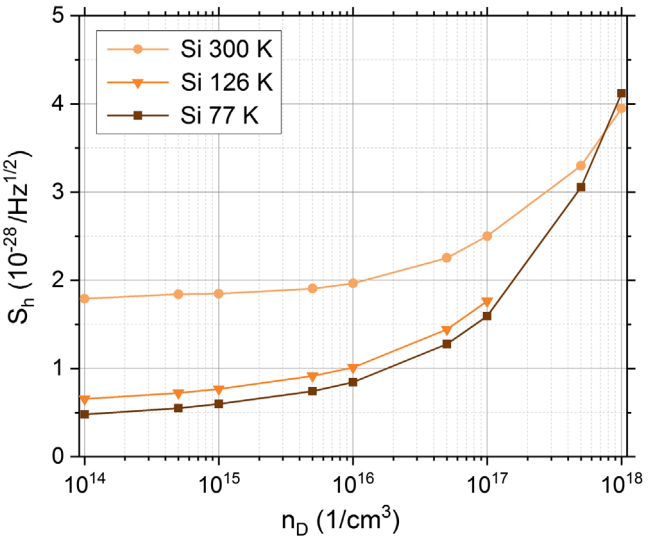

FIG. 3. Doping dependency of the ASD of TCCR noise S_h^{ξ}. At the shown temperatures, the ASD is a constant of frequency in the frequency interval of 1–10^4 Hz for Si. Because of a lack of data for the charge carrier mobility μ of doped materials at cryogenic temperatures, we show the temperatures 77, 126, and 300 K. The temperature of 126 K is interesting, because at this temperature the thermoelastic coefficient of Si vanishes, immensely reducing the thermoelastic noise. The ASD of Si at 77 and 300 K cross due to a crossing of the charge carrier mobility at high levels of doping (see Table II).

gap. Thus, the deviations from the Einstein-Smoluchowski equation are negligibly small. The mobility data for modeling D have been obtained from Jacoboni *et al.* [29] and Li and Thurber [30].

In Fig. 2, we have plotted the ASD of TCCR noise of the ET input test masses at its operation temperature of 10 K for pure Si, $n_D \approx 5 \times 10^{12}\ \frac{1}{\mathrm{cm}^3}$ using the parameters shown in Tables I and II. All numerical calculations shown have been performed with *Mathematica* 11.3 [31]. We can see that the ASD of TCCR noise at 10 K reaches $5.3 \times 10^{-30}/\sqrt{\mathrm{Hz}}$ in Si. This noise amplitude is well below the sensitivity goal of the ET of $3 \times 10^{-25}\sqrt{\mathrm{Hz}}$. Therefore, we can come to the important conclusion that TCCR noise is not a limiting noise source for the ET and third-generation gravitational wave detection, in general.

Like all thermal noise sources, TCCR noise scales with the temperature; additionally, it also increases with the doping concentration. In Fig. 3, we are showing the ASD of TCCR noise in dependence of the doping density for different temperatures. Because of the temperature range shown (77–300 K), the Debye length of Si (see Table II) is small enough to use the approximation given by formula (28), thus obtaining a frequency-independent ASD up to at least 10^4 Hz.

The doping dependence can be explained in the following way: An increase in the doping concentration increases the mean carrier concentration n_0 and decreases the Debye length ℓ_D. These effects compensate each other as can be seen in Eq. (28). Furthermore, in doped silicon ($n_D > 10^{14}\ \frac{1}{\mathrm{cm}^3}$), an increase in the doping density n_D also decreases the charge carrier mobility μ [30] and the diffusion coefficient D, respectively (see Table II), thus increasing the TCCR noise amplitude. Overall, even for room temperature (compared to cryogenic operation) and high doping densities, TCCR noise stays below the sensitivity targets of third-generation wave detectors. Calculations with other III-V semiconductors with a smaller band gap (such as gallium arsenide) have shown that the TCCR noise amplitude does not increase significantly.

IV. CONCLUSION

We show a detailed analysis of TCCR noise in metals and semiconductors from first principles especially taking into account screening effects. We show that Debye screening practically blocks diffusion processes, hence dramatically reducing TCCR noise. We apply our approach to the input masses of the Einstein Telescope and show that TCCR noise is not a limiting noise source. Furthermore, it can be seen that TCCR noise does not increase significantly at room temperature (compared to cryogenic operation) and high levels of doping of the material. For instance, for silicon input test masses of ET at room temperature and a rather high doping density of $n_D = 10^{16}\ \frac{1}{\mathrm{cm}^3}$, the TCCR noise amplitude is 3 orders of magnitude below the design sensitivity. Before this paper, the driver for ultrapure silicon has been optical absorption and TCCR noise. With our derivation, we show that TCCR noise is not a limiting noise source for substrate materials of third-generation gravitational wave detectors. Nevertheless, there is still a need for ultrapure substrate materials due to limits set by the optical absorption [21,33].

ACKNOWLEDGMENTS

S. P. V. acknowledges support from Russian Foundation of Basic Research (Grant No. 19-29-11003) and from the TAPIR GIFT MSU Support of California Institute of Technology. S. K. and F. B. acknowledge support by the German Research Foundation (DFG) under Germany's Excellence Strategy EXC-2123 QuantumFrontiers—390837967. This document has LIGO number LIGO-P2000048.

[1] B. P. Abbott *et al.*, Observation of Gravitational Waves from a Binary Black Hole Merger, Phys. Rev. Lett. **116**, 061102 (2016).

[2] B. P. Abbott *et al.* (LIGO Scientific and Virgo Collaborations), GW151226: Observation of Gravitational Waves from a 22-Solar-Mass Binary Black Hole Coalescence Phys. Rev. Lett. **116**, 241103 (2016).

[3] LVC-Collaboration, Prospects for observing and localizing gravitational-wave transients with Advanced LIGO and Advanced Virgo, Living Rev. Relativity **21**, 3 (2018).

[4] K. L. Dooley, T. Akutsu, S. Dwyer, and P. Puppo, Status of advanced ground-based laser interferometers for gravitational-wave detection, J. Phys. Conf. Ser. **610**, 012012 (2015).

[5] J. Aasi *et al.*, Characterization of the LIGO detectors during their sixth science run, Classical Quantum Gravity **32**, 115012 (2015).

[6] J. Abadie *et al.*, Advanced LIGO, Classical Quantum Gravity **32**, 074001 (2015).

[7] F. Acernese *et al.* (Virgo Collaboration), Advanced Virgo: A 2nd generation interferometric gravitational wave detector, Classical Quantum Gravity **32**, 024001 (2015).

[8] F. Acernese *et al.* (Virgo Collaboration), Calibration of Advanced Virgo and reconstruction of the gravitational wave signal h(t) during the observing run O2, Classical Quantum Gravity **35**, 205004 (2018).

[9] B. Sathyaprakash, Corrigendum: Scientific objectives of Einstein telescope, Classical Quantum Gravity **30**, 079501 (2013).

[10] S. Wills, Gravitational waves the road ahead, Opt. Photonics News **29**, 44 (2018).

[11] S. Rowan, S. Rowan, J. Hough, M. Punturo, F. Ricci, and J.-Y. Vinet, Challenges in thermal noise for 3rd generation of gravitational wave detectors, Gen. Relativ. Gravit. **43**, 593 (2011).

[12] I. W. Martin *et al.*, Effect of heat treatment on mechanical dissipation in Ta_2O_5 coatings, Classical Quantum Gravity **27**, 225020 (2010).

[13] I. Martin *et al.*, Measurements of a low-temperature mechanical dissipation peak in a single layer of Ta_2O_5 doped with TiO_2, Classical Quantum Gravity **25**, 055005 (2008).

[14] A. Zimmer *et al.*, High mechanical Q-factor measurements on silicon bulk samples, J. Phys. Conf. Ser. **122**, 012008 (2008).

[15] K. Craig *et al.*, Low temperature mechanical dissipation of an ion-beam sputtered silica film, Classical Quantum Gravity **31**, 035019 (2014).

[16] R. Nawrodt *et al.*, High mechanical q-factor measurements on calcium fluoride at cryogenic temperatures, Eur. Phys. J. **38**, 53 (2007).

[17] B. Benthem and Y. Levin, Thermorefractive and thermochemical noise in the beamsplitter of the GEO600 gravitational-wave interferometer, Phys. Rev. D **80**, 062004 (2009).

[18] P. R. Saulson, *Fundamentals of Interferometric Gravitational Wave Detectors* (World Scientific, Singapore, 1994).

[19] M. Abernathy *et al.*, Einstein gravitational wave Telescope conceptual design study, 2011, https://art.torvergata.it/handle/2108/102907?mode=simple.10#.XwRwh-dCSUl .

[20] R. A. Soref and B. R. Bennett, Electro-optical effects in silicon, IEEE J. Quantum Electron. **QE-23**, 123 (1987).

[21] J. Degallaix *et al.*, Measurement of the optical absorption of bulk silicon at cryogenic temperature and the implication for the Einstein telescope, Classical Quantum Gravity **31**, 185010 (2014).

[22] J. D. Jackson, *Klassische Elektrodynamik* (De Gruyter, Berlin, 1998).

[23] A. van der Ziel, K. M. van Vliet, and R. R. Schmidt, Temperature-fluctuation noise of thin films supported by a substrate, J. Appl. Phys. **51**, 2947 (1980).

[24] M. L. Gorodetsky, V. B. Braginsky, and S. P. Vyatchanin, Thermodynamical fluctuations and photo-thermal shot noise in gravitational wave antennae, Phys. Lett. A **264**, 1 (1999).

[25] L. L. Landau and E. M. Lifshitz, *Theoretical Physics: Statistical Physics* (Butterworth-Heinemann, London, 1980), Vol. 5.

[26] A. Chintchin, Korrelationstheorie der stationären stochastischen prozesse, Math. Ann. **109**, 604 (1934).

[27] D. Forster, *Hydrodynamic Fluctuations, Broken Symmetry, and Correlation Functions* (CRC Press, Boca Raton, FL, 1975).

[28] M. Grundmann, *The Physics of Semiconductors* (Springer, New York, 2016).

[29] C. Jacoboni, C. Canali, G. Ottaviani, and A. Alberigi Quaranta, A review of some charge transport properties of silicon, Solid State Electron. **20**, 77 (1977).

[30] S. S. Li and W. Robert Thurber, The dopant density and temperature dependence of electron mobility and resistivity in n-type silicon, Solid State Electron. **20**, 609 (1977).

[31] Wolfram Research, Inc., Mathematica, Version 11.3.

[32] C. Schinke *et al.*, Uncertainty analysis for the coefficient of band-to-band absorption of crystalline silicon, AIP Adv. **5**, 067168 (2015).

[33] A. Rüdiger, W. Winkler, K. Danzmann, and R. Schilling, Heating by optical absorption and the performance of interferometric gravitational-wave detectors, Phys. Rev. A **44**, 7022 (1991).